Isolation and Characterization of a Porous Carbonate Apatite From Porcine Cancellous Bone

Shu-Tung Li, Ph.D., Hui-Chen Chen, Ph.D., Debbie Yuen

Science, Technology, Innovation, Aug. 2014: 1-13

Isolation and Characterization of a Porous Carbonate Apatite From Porcine Cancellous Bone

Shu-Tung Li, Ph.D., Hui-Chen Chen, Ph.D., Debbie Yuen

Abstract Animal derived Porous Carbonate Apatite (PCA), commonly referred to as Anorganic Bone Mineral, was isolated from porcine cancellous bone using a combination of chemical and heat treatments. This article summarizes the results of *in vitro* and *in vivo* studies conducted for PCA. *In vitro*, the structure of PCA was characterized by X-Ray diffraction (XRD) and Fourier Transform Infrared (FTIR) Spectroscopy, the pore structure of the PCA particles was analyzed from images obtained from scanning electron microscopy (SEM), the particle size distribution as well as the volume fill per unit weight of PCA were also determined. *In vivo*, two studies were conducted using a rabbit femoral condyle bone defect model and canine intraoral one-wall defect model to evaluate the safety and effectiveness of PCA as a bone grafting material. A commercial product of Carbonate Apatite derived from bovine bone, Bio-Oss® (Geistlich-Pharma, Switzerland), was also characterized for comparison. In summary, *in vitro* studies demonstrated that PCA fulfills the physical, structural and morphological requirements needed to function as an effective bone grafting material. *In vivo* studies from rabbit femoral condyle defect model and canine intraoral bone defect model demonstrated that PCA functioned as well as Bio-Oss® in both the orthopedic bone defect and the intraoral bone defect as an osteoconductive matrix to support bone regeneration.

Introduction

Carbonate Apatite isolated from bovine bone, also known as anorganic bovine bone mineral (e.g., Bio-Oss®), has been in commercial distribution for bone grafting applications for more than a decade, particularly in dental surgeries. Advantages of these materials over the synthetic calcium phosphate materials (e.g., β-tricalcium phosphate and hydroxyapatite) are many. Carbonate Apatite derived from natural bone has a structure similar to that of the native bone mineral and, therefore, would remodel close to the native bone mineral *in vivo*. Since Porous Carbonate Apatite (PCA) is isolated from the cancellous bone of porcine bone, it possesses the natural pore structure for cell conduction. Further, because the apparent density of PCA is low, the intra- and inter-particle space is high for osteo-conduction and new bone deposition.

In this article we present results of *in vitro* and *in vivo* studies of a newly developed natural carbonate apatite isolated from porcine cancellous bone. The structure of the PCA was characterized from x-ray diffraction of PCA particles and the carbonate content of PCA was determined from Fourier Transform Infrared Spectroscopy. The pore sizes and their distribution were determined from scanning electron micrographs of PCA particles. Particle size distribution of a given product sample as well as the volume fill capacity per unit weight of PCA particles were also analyzed. The results of the *in vitro* and *in vivo* studies were compared to the Bio-Oss® particles.

Materials and Methods

Porous Carbonate Apatite

Fresh porcine cancellous bone was obtained from a local abattoir. The adhering tissues including the surrounding cartilage were removed. The bone was then ground into particles of 10mm to 15mm in size. After thorough rinsing with water to remove blood and water soluble proteins, the particles were subjected to a proprietary combination of chemical and heat treatment to remove most if not all organic materials from the bone, resulting in a highly purified carbonate apatite with minimal distortion of the intact geometry of the mineral phase from the original bone.

Scanning Electron Microscopy (SEM)

Scanning electron micrographs (JEOL Ltd, JSM 5800 Scanning Electron Microscope) were obtained to examine the morphology and the pore structure for the respective particles of PCA and Bio-Oss®. The particles were evaluated under X25, X50 and X75 magnifications. Multiple images were taken for the evaluation of the pore sizes and their distribution.

X-Ray Diffraction (XRD)

X-Ray diffraction analysis was conducted using PHILIPS PW 1710 X-ray diffractometer, scanning at a rate of

Address for Correspondence:
Collagen Matrix, Inc.
15 Thornton Road
Oakland, NJ 07436, USA, (www.collagenmatrix.com)

0.01° 2θ per second. Approximately 100mg of each of powdered samples of PCA and Bio-Oss® was placed on a sample holder and scanned from 20 to 40 degrees (2θ scale) to obtain key reflections for the identification of the structure.

Fourier Transform Infrared Spectroscopy (FTIR Spectroscopy)

FTIR spectroscopy analysis was conducted using Perkin Elmer 983G FTIR spectrophotometer to determine the functional groups and carbonate content. Samples were prepared as KBr pellets which contain 10% (w/w) of minerals.

Pore Structure of the Mineral Particles

The pore sizes of mineral particles were measured from SEM micrographs. Pore size was defined as the longest distance of a pore.

Particle Size Distribution

A fixed weight of the mineral particles was passed through different sizes of meshes and the weight of the particles collected within different size ranges of mesh was determined.

Volume Fill Measurement

A unit weight (1g) of mineral material was poured into a small volumetric cylinder and the volume occupied by the mineral was recorded.

Animal Study

Rabbit Femoral Condylar Bone Defect Model

The surgery was conducted at IBEX Preclinical Research, Inc. (Logan, UT), and histology processing and analysis were conducted at Histion (Everett, WA) under approved protocols. Eighteen female New Zealand White rabbits were divided into 2 groups (6 implants per group and per time point). Each group of rabbits underwent general anesthesia and aseptic surgery to create a bilateral defect (approximately 5mm diameter and 6-8mm deep) in the lateral femoral condyles. Defects were filled with either PCA or Bio-Oss® implants in contra-lateral defects according to the experimental design. The surgical wound was closed and the rabbits were recovered and monitored daily for 4, 8 and 14 weeks. Radiographs were taken before sacrifices at each time point. A necropsy was performed to grossly assess each implant and the operative sites were harvested. Explanted femurs were placed in 10% formalin solution, fixed for several days and then shipped to the histology laboratory.

Canine Intraoral Bone Defect Model

The study was conducted at NAMSA (Northwood, OH). Twelve male beagle dogs had the third pre-molars (P3) extracted from the mandible. After 14 weeks post-extraction, the defect creation procedure was initiated. Each animal had a defect created (4mm width x 5mm depth) at the distal aspect of the 2nd premolars and the mesial aspect of the 4th premolars to yield four mandibular defect sites per dog. The defects were then treated with either PCA or Bio-Oss® (18 sites per article). After treatment, a commercial marketed collagen dental membrane was placed over treated defect sites. Animals were observed daily for general health and gingival health weekly. Body weights were taken pre-operatively and weekly thereafter. Radiographs of defects sites were taken for 4, 8 and 12 weeks. Explanted sites were harvested, fixed, and processed for microscopic and histological evaluation.

Histological Processing and Histology Evaluation

Rabbit Femoral Condylar Bone Defect Model

Specimens were trimmed, embedded in methyl methacrylate (MMA), and were randomized for evaluation. Radiographs were taken of each specimen prior to embedding in MMA to facilitate visualization of the residual implant materials and newly-formed bone within the defects. Goldner's trichrome-stained sections taken through the long axis of each defect were evaluated for percent new bone formation (calcified tissue), percent of bone marrow and percent of residual implant. Hematoxylin and eosin (H&E) stained sections taken in parallel planes were evaluated for inflammation and giant cells (GCs) to determine the cellular response to the implants. Scores for bone and bone marrow were added to produce a total bone score for each specimen. Scores for inflammation and giant cells were added to produce a total cellular score.

All sections were evaluated, blind to treatment, by a single evaluator using the semiquantitative scoring system developed by the histology lab and provided in Table 1. Once semiquantitative analysis was completed, the evaluator was un-blinded and all sections were grouped and compared. Median scores ± standard errors of the mean were calculated for each group. Differences between groups were determined with the Kruskal-Wallis multiple comparisons test using STATISTICA (Version 9).

Table 1: Semiquantitative Analysis Scoring System for Rabbit Femoral Condylar Bone Defect Model

Bone (Calcified Tissue)	***Score***	***Giant Cells***	***Score***
Occupies 76-100% of implant area	5	Extensive (Large numbers throughout the implant area)	4
Occupies 51-75% of implant area	4	Moderate numbers (multiple foci or much in one area)	3
Occupies 26-50% of implant area	3	Small numbers (occasional foci)	2
Occupies 10-25% of implant area	2	Very small amount in 1 or 2 small focal areas	1
Occupies <10% of implant area	1	None	0
None	0		
Bone Marrow	***Score***	***Inflammation***	***Score***
Occupies 76-100% of implant area	5	Extensive (Large numbers throughout the implant area)	4
Occupies 51-75% of implant area	4	Moderate numbers (multiple foci or much in one area)	3
Occupies 26-50% of implant area	3	Small numbers (occasional foci)	2
Occupies 10-25% of implant area	2	Very small amount in 1 or 2 small focal areas	1
Occupies <10% of implant area	1	None	0
None	0		
Total Possible Bone Score	**10**	**Total Possible Cellular Score**	**8**

Residual Bone Mineral	***Score***
Occupies 76-100% of implant area	5
Occupies 51-75% of implant area	4
Occupies 26-50% of implant area	3
Occupies 10-25% of implant area	2
Occupies <10% of implant area	1
Total Possible Residual Implant Score	**5**

Canine Intraoral Bone Defect Model

A board certified veterinary pathologist performed the microscopic/histologic examination using incandescent and polarized light microscopy. Tissue sections stained with hematoxylin and eosin (H&E) were used to evaluate the cellular response (i.e. inflammation, giant cells, lymphocytes, plasma cells, macrophages, necrosis, neovascularization, fibrosis and fatty infiltrate) following the scoring criteria (0 = absent; 1 = minimal/slight; 2 = mild, 3 = moderate and 4 = marked/severe) described in the ISO-10993, Part 6. Scores for cellular response were each added together to produce tissue response scores for each specimen and averaged scores were calculated based on the total number of specimens per group. Tissue sections stained with Masson's trichrome stain were evaluated for bone healing activity and scored according to the scoring system described in Table 2. Once histology analysis was completed, all sections were grouped and compared. Median scores ± standard deviation of the mean were calculated for treated groups.

Table 2: Semiquantitative Analysis Scoring System for Canine Intra-oral Bone Defect Model

Parameters	*Description*	*Score*
Lamellar Bone Regeneration	Regeneration not evident	0
	Some regeneration is evident	1
	Regeneration is evident but not complete	2
	Regeneration appears complete	3
Woven Bone Regeneration	Regeneration not evident	0
	Some regeneration is evident	1
	Regeneration is evident but not complete	2
	Regeneration appears complete	3
Residual Implant Material	No material is evident	0
	Some material is present	1
	Much of the material is evident	2
	All of the materials appears to be present	3

Results

In Vitro Characterization Data

Scanning Electron Microscopy (SEM)

Figure 1a and 1b show SEM micrographs of PCA and Bio-Oss® at three different magnifications, respectively. SEM revealed the porous structure of PCA and Bio-Oss®. Both PCA and Bio-Oss® showed interconnecting pores but this was more manifested in PCA than in Bio-Oss®. It can be seen from the micrographs that PCA compares favorably against Bio-Oss® in terms of pore structure within the particles. It was also noted that the surface appears to be rougher in the PCA than in the Bio-Oss®, a property favoring the cell adhesion to PCA particles.

Figure 1a: SEM Micrographs of Porous Carbonate Apatite (PCA)

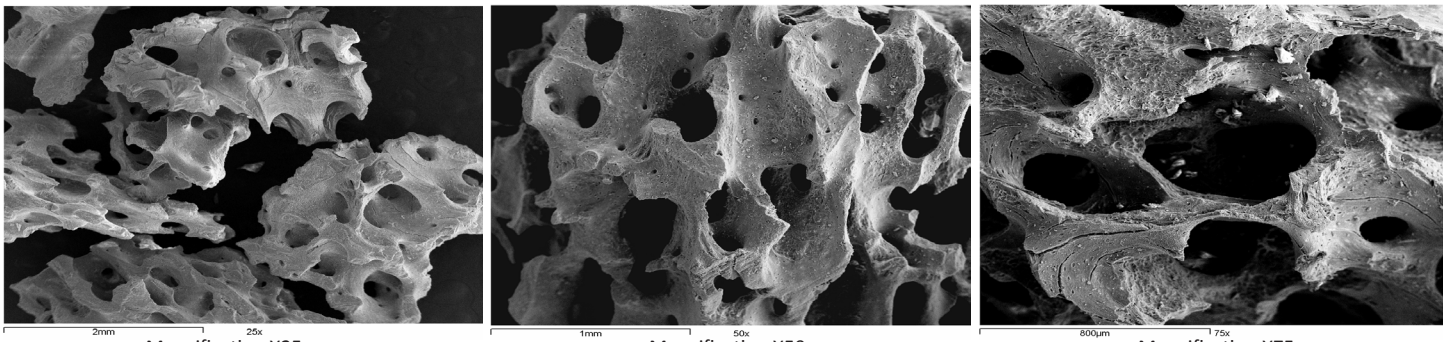

Magnification X25 Magnification X50 Magnification X75

Figure 1b: SEM Micrographs of Bio-Oss®

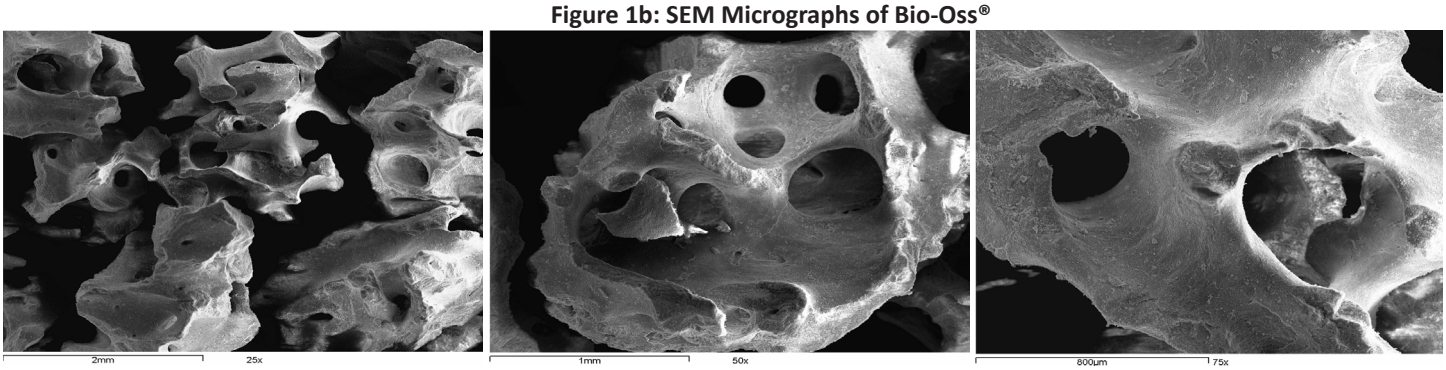

Magnification X25 Magnification X50 Magnification X75

X-Ray Diffraction

The diffraction pattern of PCA and Bio-Oss® in terms of the key mineral reflections and the peak broadening profile of the respective mineral reflections are shown in Figure 2 below. The X-ray diffraction pattern of PCA is almost identical to that observed for Bio-Oss®. Both diffraction patterns are close to the mature native bone diffraction pattern that is consistent with bone mineral of apatite nature with low degree of crystallinity. [1]

Figure 2: X-Ray Diffraction Pattern of PCA and Bio-Oss®

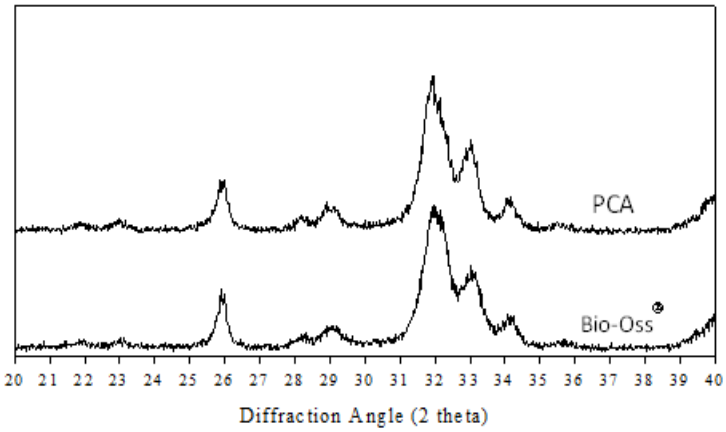

Fourier Transform Infrared Spectroscopy (FTIR Spectroscopy)

As seen from the FTIR spectra in Figure 3, the major IR absorption peaks for PCA and Bio-Oss® are consistent with the mature bone mineral structure, including the phosphate ion bands (sharp P-O, anti-symmetrical bending mode, 550cm^{-1} to 600cm^{-1}; anti-symmetrical stretching mode, 1030cm^{-1} with 1100cm^{-1} shoulder) and carbonate ion (CO_3) band (anti-symmetrical stretching mode, 1400cm^{-1} - 1500cm^{-1}), and the carbonyl (CO).

Figure 3: IR Spectra of PCA and Bio-Oss®

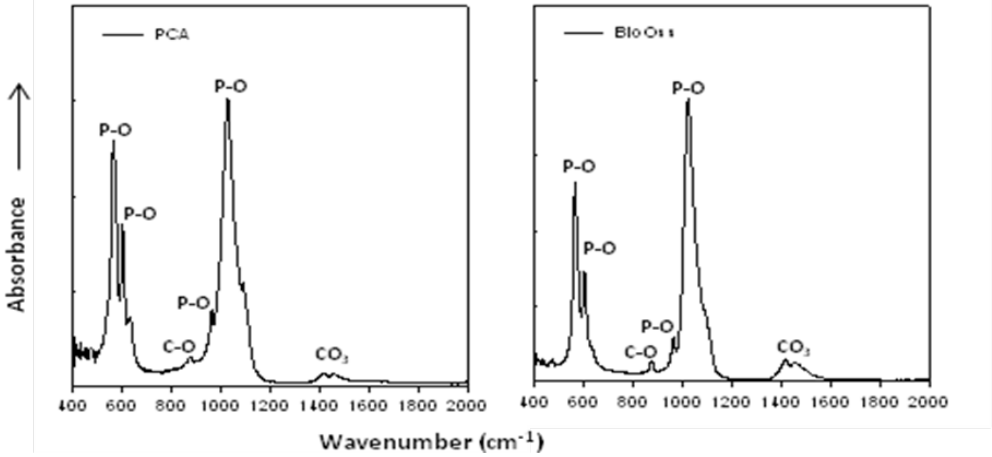

Pore Structure of the Particles

Figure 4 below summarizes the pore size distribution for the PCA and Bio-Oss® particles of comparable range of sizes. The majority of macropores for PCA and Bio-Oss® are in the range of 0.1mm to 1.0mm.

Figure 4: Pore Size Distribution Plot of PCA and Bio-Oss®

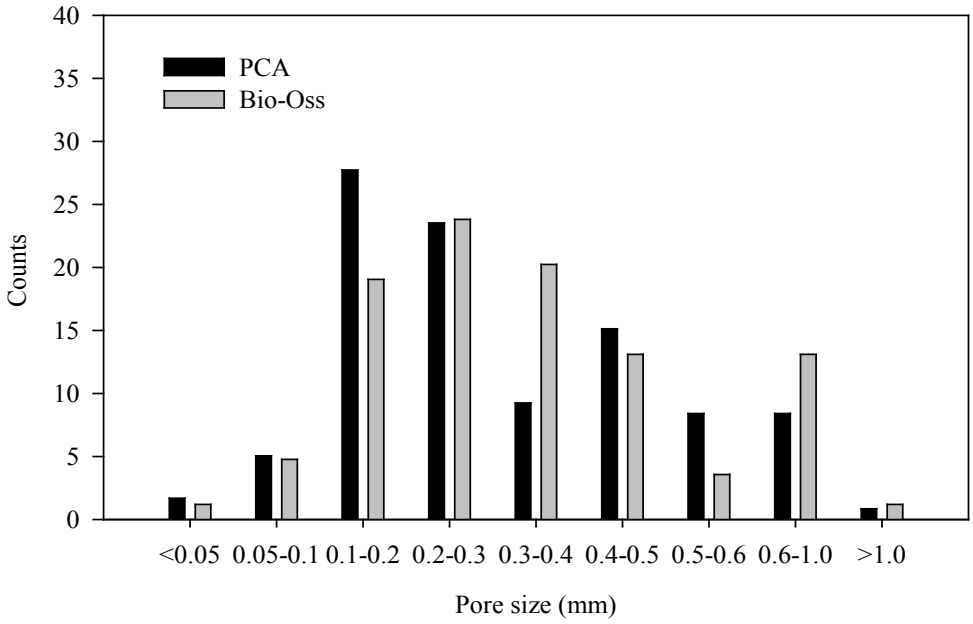

Particle Size Distribution

Figure 5 below summarizes the results of particle size distribution studies. As seen from the figures within the same particle size range of each product, the PCA has a higher percentage of larger size of particles than Bio-Oss®. This is more manifested when the range of the particle sizes increases. As will be seen in the next section, particle size distribution affects the volume fill capacity and the volume available for new bone deposition. The higher percentage of larger particles will result in a higher number of intra-particle pores and intra-particle spaces that can have additional benefit for bone conduction and growth.

Figure 5: Particle Size Distribution Plots of PCA and Bio-Oss®

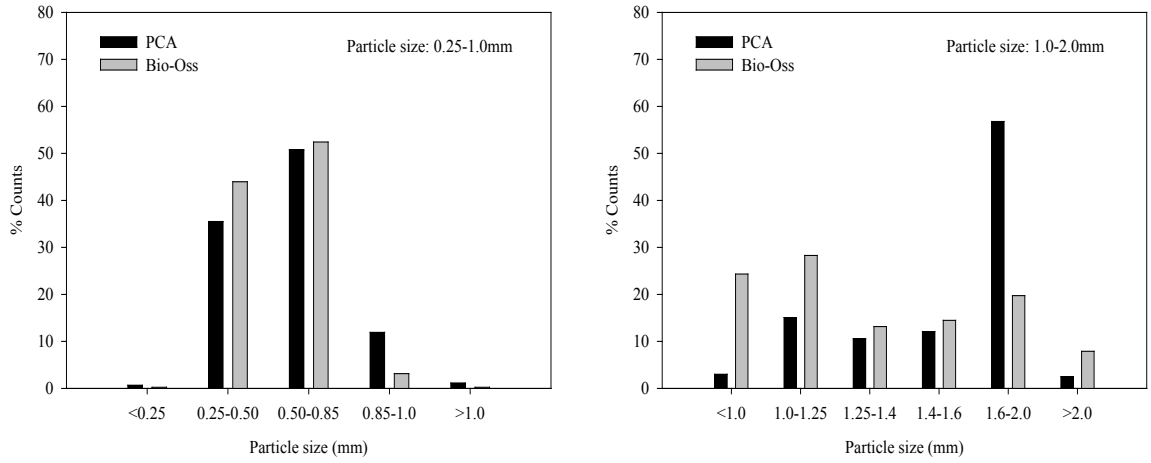

Volume Fill Capacity

Volume fill per unit weight of bone mineral relates to the empty space available for new bone growth *in vivo*. A unit weight (1g) of mineral material was slowly poured into a small volumetric cylinder and the volume occupied by the mineral was recorded and compared between PCA and Bio-Oss®. Table 3 below summarizes the results of volume fill measurements.

Table 3: Volume Fill Measurements and % Void Space of PCA and Bio-Oss®

	Volume Fill Measurements		% Void Space	
Products	Particle Size 0.25-1.0mm*	Particle Size 1.0-2.0mm*	Particle Size 0.25-1.0mm*	Particle Size 1.0-2.0mm*
PCA	2.86 ± 0.13 cm^3/g	4.35 ± 0.34 cm^3/g	88%	95%
Bio-Oss®	2.13 ± 0.08 cm^3/g	2.91 ± 0.08 cm^3/g	78%	88%

*Results represent an average of 5 measurements ± SD

For both particle sizes of 0.25-1.0mm and 1.0-2.0mm, PCA has a statistically significant higher volume fill capacity than Bio-Oss®. As an example, to fill a 1cc volume of bone defect, PCA only occupies a volume of about 0.12cc and 0.88cc will be empty for new bone deposition if the particle size is in the range of 0.25-1.0mm. The percent volume fill of PCA increases significantly with increasing particle size, being 34% over Bio-Oss® for small particle size range and 49% over Bio-Oss® for large particle size range, respectively. The data indicates that PCA provides more intra- and inter-particle space for osteoconduction and new bone deposition than Bio-Oss®. This observation is consistent with SEM micrographs which show more porous structure of PCA than Bio-Oss®.

***In Vivo* Animal Studies**

Rabbit Femoral Condylar Bone Defect Study

Semiquantitative Analysis

Individual semiquantitative data from each slide of PCA and Bio-Oss® were collected and the median results determined for the individual parameters. Total bone score (calcified bone + bone marrow) and total cellular responses (inflammation + giant cells) are summarized in Table 4 below.

Table 4: Semiquantitative Histological Analysis Results in Rabbit Femoral Condylar Model

Group	Time Point	Calcified Bone	Bone Marrow	Residual Implant	Inflammation	Giant Cells	Total Bone Score	Total Cellular Response
PCA	4 weeks	3.0±0.0	3.0±0.2	3.0±0.2	0.00±0.0	1.0±0.5	6.0±0.2	1.0±0.5
	8 weeks	3.0±0.2	3.5±0.3	3.0±0.3	0.00±0.0	0.5±0.3	6.5±0.4	0.5±0.3
	14 weeks	3.0±0.0	3.0±0.2	3.0±0.2	0.00±0.2	0.5±0.4	6.0±0.2	0.5±0.4
Bio-Oss®	4 weeks	3.0±0.0	2.5±0.2	3.5±0.2	0.00±0.0	1.0±0.2	5.5±0.2	1.0±0.2
	8 weeks	2.5±0.2	3.5±0.2	3.0±0.4	0.00±0.0	0.0±0.2	6.0±0.3	0.0±0.2
	14 weeks	3.0±0.2	3.0±0.3	3.0±0.3	0.00±0.0	1.0±0.2	6.0±0.3	1.0±0.2

There was no significant difference in percent residual implant material, inflammation or giant cells between PCA and Bio-Oss® groups at any time point. However, there is a slight increase of the total bone content in the PCA group over the Bio-Oss® group between 4- and 8-weeks with no significant difference between the 8- and 14-week time points.

Qualitative Analysis

Representative histology images of PCA treated and Bio-Oss® treated groups at 4-week and 14-week time points are shown in the Figure 6.

Figure 6: Histology of PCA and Bio-Oss® treated groups at 4 and 14 weeks in Rabbit Femoral Condylar Model (70X magnification, Goldner's Trichrome Stain)

4 Weeks: PCA

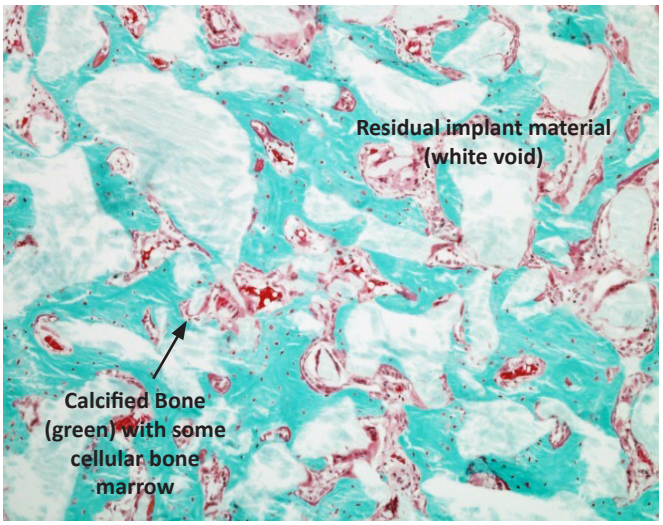

4 Weeks: Bio-Oss®

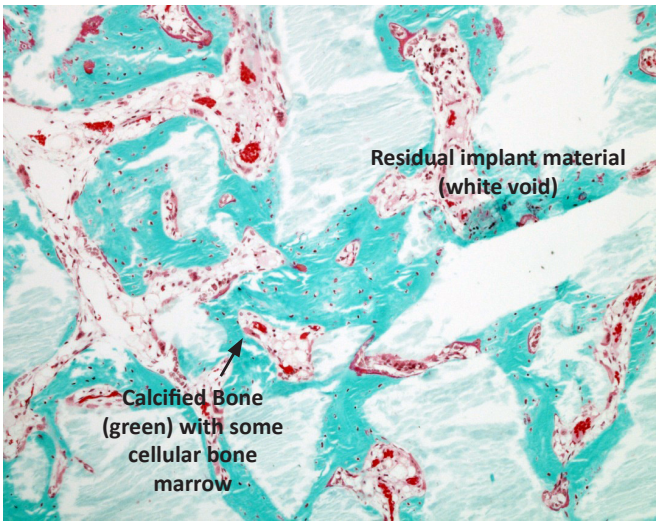

14 Weeks: PCA

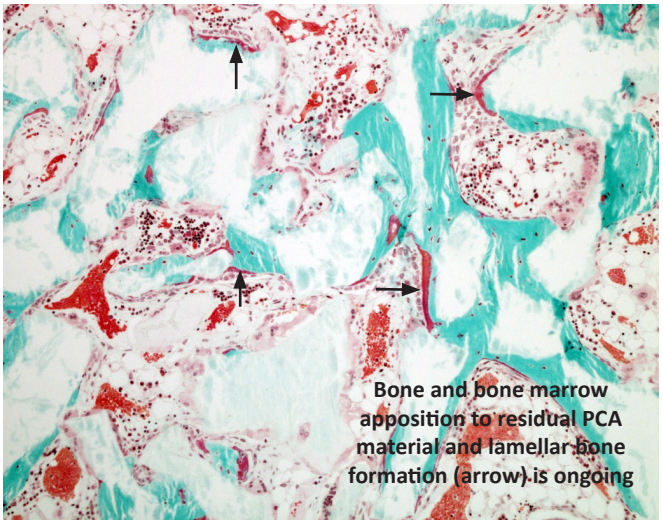

14 Weeks: Bio-Oss®

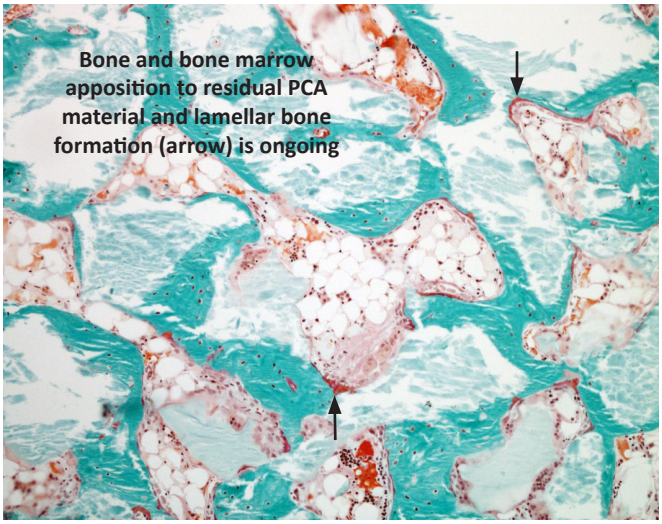

At 4 weeks in the PCA group, newly-formed calcified bone and a small amount of bone marrow were seen apposed to the surfaces of the residual PCA material. A small amount of lamellar bone formation was ongoing at focal areas at the peripheral portion as well as within the central portion of the residual masses. At 14 weeks, slightly more cellular bone marrow was evident in sections from the PCA implanted group compared to the Bio-Oss® control group. In addition, slightly more lamellar bone formation was ongoing throughout the defects and small amount of intramembranous bone

formation was seen at occasional sites found adjacent to residual implant materials. No chronic or acute inflammation was observed from all sections.

Similar to PCA implanted group, residual Bio-Oss® material could be found dispersed throughout the majority of the defect space in all sections at 4 weeks. Predominantly newly-formed calcified bone and some bone marrow were seen apposed to the surfaces of the residual implant material. A small-to-moderate amount of lamellar bone formation was ongoing at focal areas at the peripheral portion as well as within the central portion of the residual implant masses.

At 14 weeks, residual Bio-Oss® implant material was still found. Newly-formed calcified bone and/or fatty bone marrow was seen apposed to the surfaces of the residual implant material. Lamellar bone formation was still ongoing at focal areas throughout the residual mass. The amount of ongoing bone formation was comparable to that seen at earlier time points. No chronic or acute inflammation was seen in any of the sections.

Overall, qualitative evaluation showed that ongoing bone formation and resorption was similar for both groups over time. There was slightly more cellular bone marrow and slightly increased numbers of osteoclasts were found on surfaces of newly-formed bone present on the residual PCA material between 8 and 14 weeks that was not observed for the Bio-Oss® group, an observation consistent with rougher morphological surface of the PCA particles as compared to Bio-Oss®. Slightly more lamellar bone formation within the defect was also seen at 14 weeks for the PCA treatment group compared to the Bio-Oss® group.

Canine Intraoral Bone Defect Model

Radiographs

Representative post-operative defect and post-operative treatment radiographs taken from PCA and Bio-Oss® implanted group at each time point are shown in Figure 7.

Figure 7a: Representative Radiograph Images of PCA Treated Defects in Canine Intraoral Model

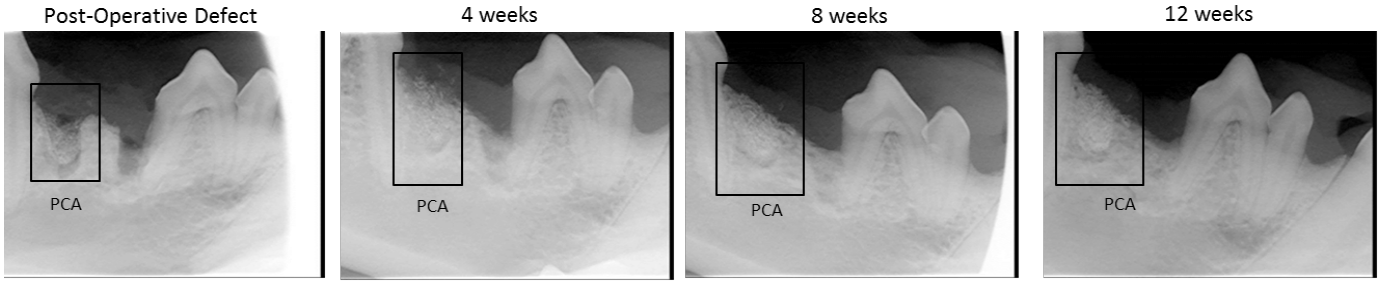

Figure 7b: Representative Radiograph Images of Bio-Oss® Treated Defects in Canine Intraoral Model

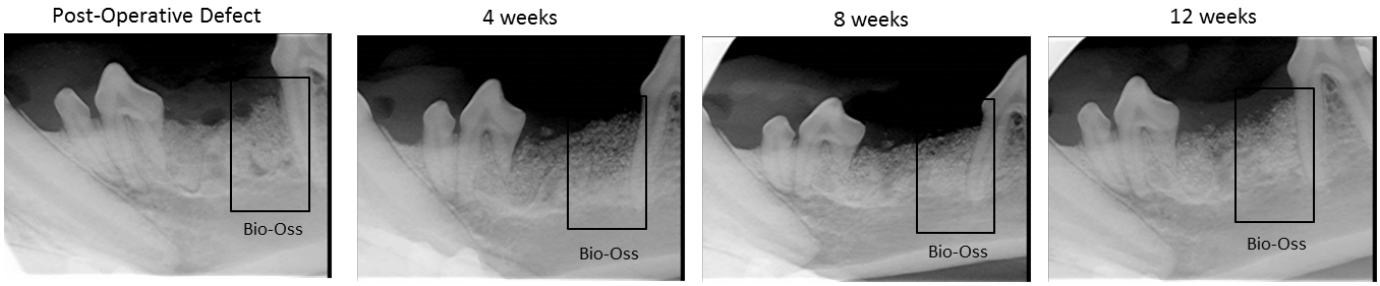

At 4 weeks, the Bio-Oss® defect sites showed a lack of increase in radiodensity, suggesting minimal bone formation as compared to the defect sites treated with PCA. At 8 weeks, the PCA treated sites appeared to have generated a greater interradicular bone pattern, compared to the site treated with Bio-Oss®. By 12 weeks post-treatment, defect sites had become difficult to distinguish radiographically from surrounding bone due to new bone formation within the defect with remodeling and associated article absorption. For PCA treated sites, noticeably increased radiodensity and development of interradicular bone by the 12-week post treatment was observed as compared to previous time points. The Bio-Oss® treated sites as compared to the PCA treated sites, showed less bone development based on overall radiolucencies.

Microscopic/Histology Analysis

Average of individual histological score data from the defect sites treated with PCA and Bio-Oss® were collected and are summarized in Table 5. Representative histology micrographs of the defect sites treated with either the PCA or Bio-Oss® are shown in Figures 8 and 9.

Table 5: Results of Microscopic/Histology Analyses in Canine Intraoral Model

Group	Time Point	Lamellar Bone Regeneration	Woven Bone Regeneration	Residual Implant Material	Tissue Response
PCA	4 weeks	1.2 ± 0.4	1.5 ± 0.5	2.0 ± 0.0	9.0 ± 4.5
	8 weeks	1.5 ± 0.5	2.0 ± 0.0	2.0 ± 0.0	7.2 ± 0.4
	12 weeks	2.0 ± 0.0	2.0 ± 0.0	1.8 ± 0.4	6.7 ± 2.0
Bio-Oss®	4 weeks	1.2 ± 0.4	1.3 ± 0.5	1.7 ± 0.5	7.8 ± 1.3
	8 weeks	1.3 ±0.5	1.7 ± 0.5	1.8 ± 0.4	7.7 ± 2.7
	12 weeks	2.0 ± 0.0	1.8 ± 0.4	2.0 ± 0.0	6.7 ± 1.5

Microscopically, implantation of the PCA and Bio-Oss® supported bone regeneration and healing. Over the duration of the study the total amount of bone increased, and the proportion of mature lamellar bone increased relative to the immature woven bone. There was no apparent difference in the total amount of bone formed within the sites treated with either the PCA or Bio-Oss®. The amount of implant material remaining with each group was similar as well as the amount of implant material decreased with time over the duration of the study. Histologically, PCA and Bio-Oss® elicited similar tissue responses, and the PCA was considered a nonirritant at all intervals, suggesting that there was no evidence of a safety issue associated with implantation of PCA.

Figure 8: Histology of PCA treated group vs. Bio-Oss® treated group at 4, 8 and 12 weeks in Canine Intraoral Model (20X magnification, H&E Stain)

4 Weeks: PCA

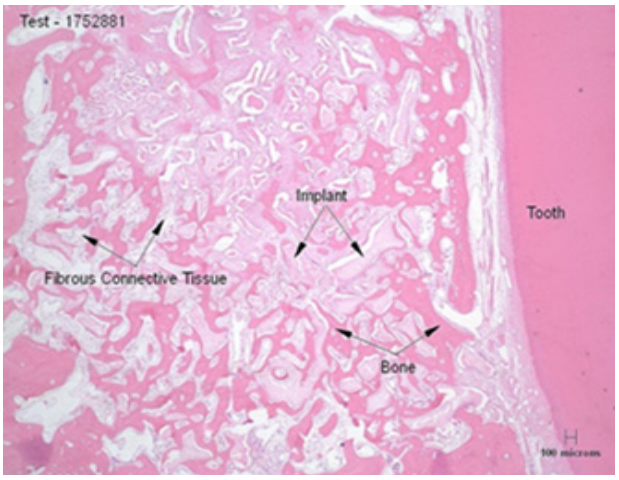

4 Week: Bio-Oss®

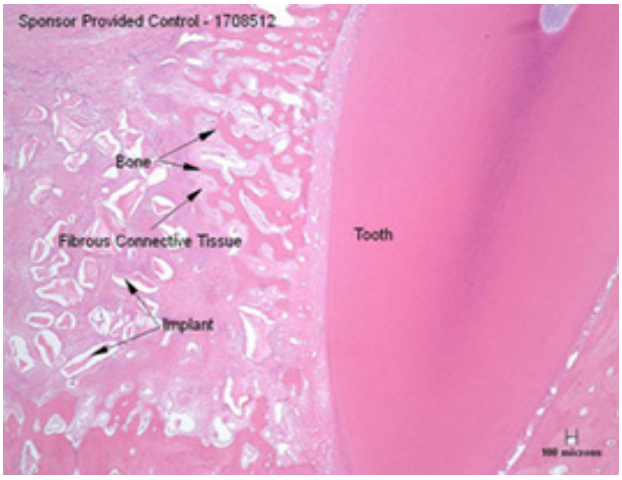

8 Weeks: PCA

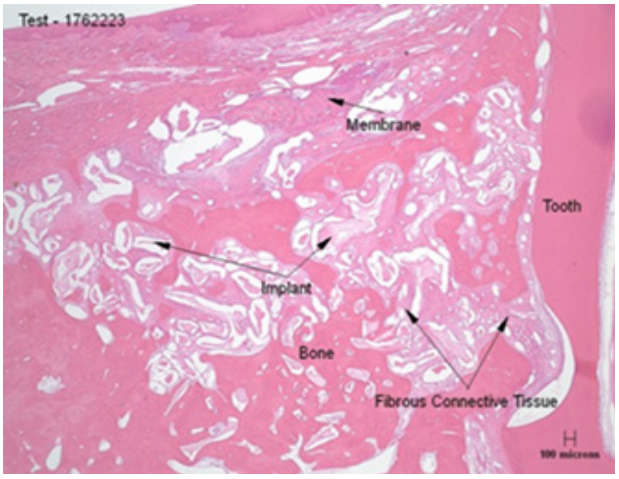

8 Weeks: Bio-Oss®

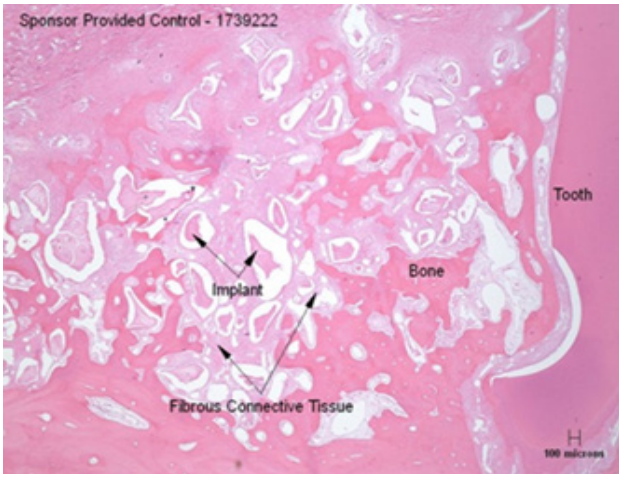

12 Weeks: PCA

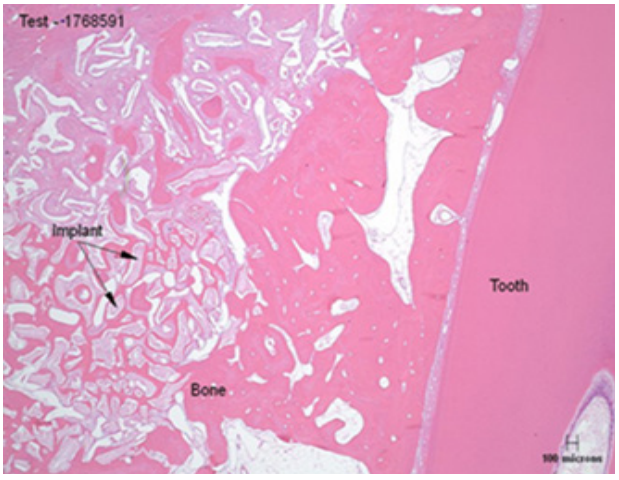

12 Weeks: Bio-Oss®

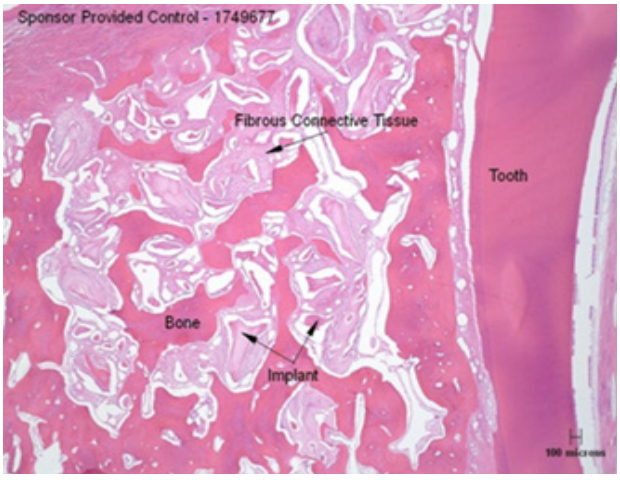

Figure 9: Histology of PCA treated group vs. Bio-Oss® treated group at 4, 8 and 12 weeks in Canine Intraoral Model (20X magnification, Masson's trichrome Stain)

4 Weeks: PCA

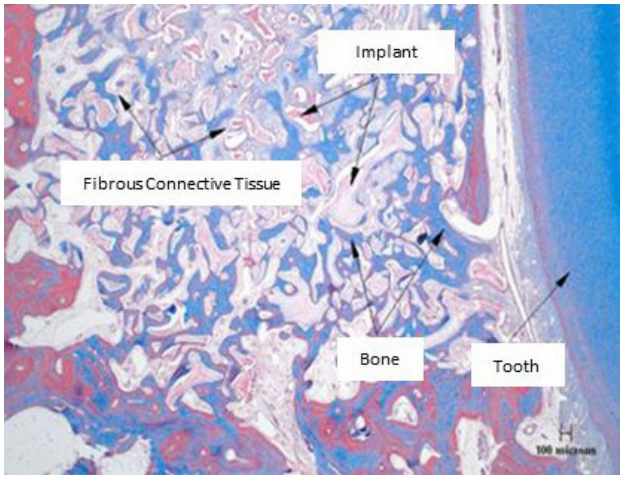

4 Weeks: Bio-Oss®

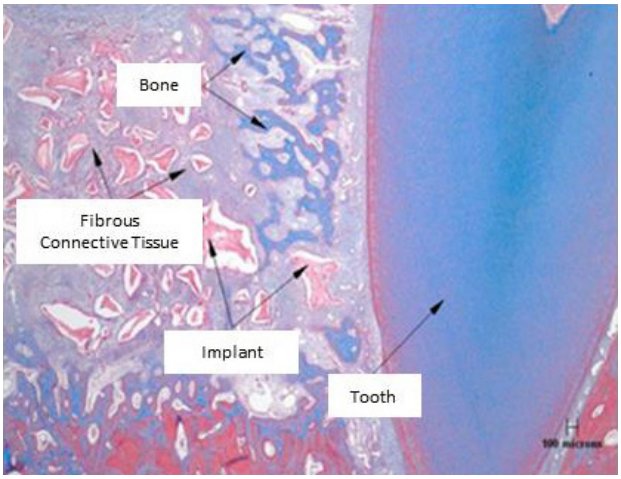

8 Weeks: PCA

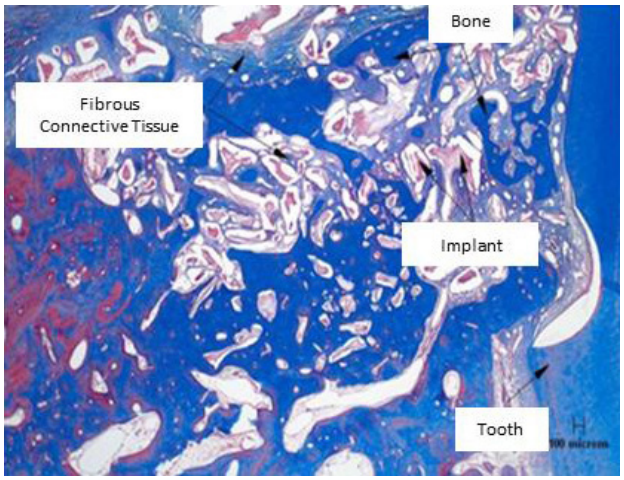

8 Weeks: Bio-Oss®

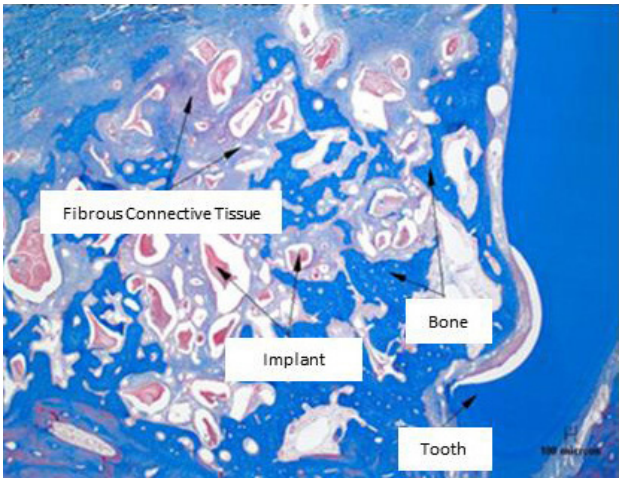

12 Weeks: PCA

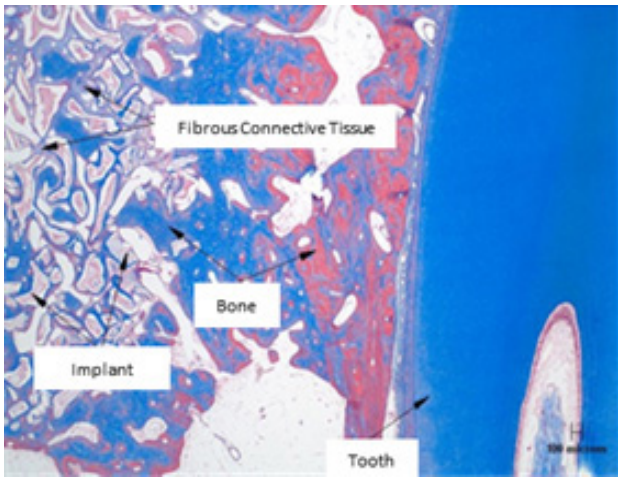

12 Weeks: Bio-Oss®

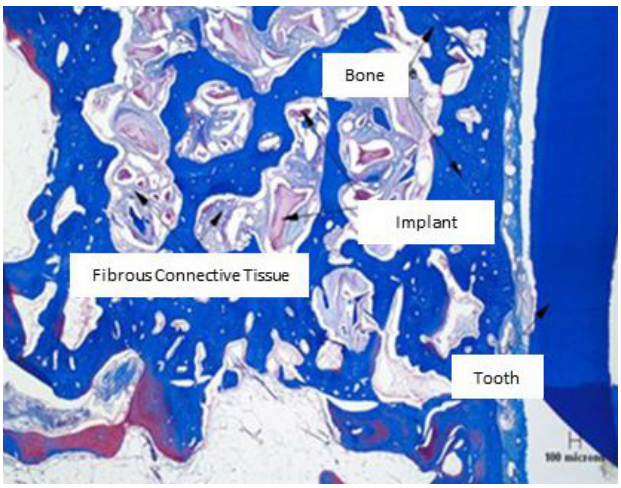

Discussion

Calcium-containing minerals currently on the market for bone grafting applications are generally osteo-conductive. The relative extent of osteo-conductivity of these materials has not been fully elucidated. The general consensus in the field is that the material should be resorbable and the rate of resorption should balance the rate of new bone deposition such that there will not be any slumping of the material due to premature resorption. In addition, the material should have interconnecting pores with pore size in the range of 150µm to about 600µm for which cells can infiltrate into the porous structure for effective osteo-conduction and bone biosynthesis.[2] Furthermore, the material should not occupy a large portion of the bone void space which can interfere with osteoblast cell growth, multiply and new bone deposition and remodeling. Lastly, the surface of the material should be rough at microscopic level to facilitate cell adhesion and migration.

Given the material requirements cited above, many materials on the market will not fulfill all the requirements for an ideal osteo-conductive bone graft material. For example, on the one end of the resorption scale, calcium sulfate, a commonly used material for bone grafting, resorbs quickly *in vivo* (3-4 weeks) resulting in material slumping and incomplete bone regeneration or bone fill, whereas on the other end of the scale, hydroxyapatite, a highly crystalline calcium phosphate based material, is a very slow resorbing material *in vivo* (years). Once implanted, hydroxyapatite will remain in the bone void and mingle with the regenerated bone mineral. A key disadvantage of hydroxyapatite implant is that the implant material is randomly distributed within the regenerated bone matrix which can interfere with the remodeling process of the natural bone since the natural bone *in vivo* is organized with respect to the functional requirements of the tissue at a particular anatomic site.

Another requirement is related to the pore structure of the material. Highly porous material serves a dual function for bone grafting. It provides a high degree of osteo-conductivity and yet minimizes the amount of implant material or the residual implant material left behind post bone regeneration. Both of these properties are highly desirable in designing a bone graft material to guide the bone regeneration *in vivo*. Given that described above, one would think that if there is a way to isolate the bone mineral component from cancellous bone without significantly changing its macroscopic morphology and the microscopic structure, the material would satisfy all the requirements for bone grafting applications. In this regard, it was noted that PCA is more porous than the Bio-Oss®. As a result, there will be more space available for new bone deposition in PCA over Bio-Oss®. One other characteristic which benefits PCA over Bio-Oss® is the surface morphology. The rougher surface of PCA would facilitate cell adhesion and spread for bone growth than the Bio-Oss®. This observation is correlated with a higher *in vivo* activity of osteoblasts that resulted in more bone marrow and lamellar bone formation at early time points.

Many animal and clinical studies have been conducted on Bio-Oss® and the material has been well accepted in the dental community for its safety and effectiveness for oral surgical applications in periodontal and guided bone regeneration procedures. Numerous studies have been published for Bio-Oss® over the past decade. Based on the results of *in vitro* and *in vivo* studies provided in this article, it is anticipated that PCA will function at least as well as Bio-Oss® if not better in the clinical environment for intraoral bone grafting applications.

REFERENCES

1. Tadic D. Epple M. A Thorough Physiochemical Characterization of 14 Calcium Phosphate Bone Substitution Materials in Comparsion to Natural Bone. Biomaterials. 2004; 25 (6): 987-994.

2. Figueiredo M. et al. Physicochemical Characterization of Biomaterials Commonly Used in Dentistry as Bone Substitutes - Comparsion with Human Bone. J. Biomed Mater. Res. Part B:Appl. Bio Mater 92B:409-419, 2010.